ePublishing

EKT ΕΘΝΙΚΟ ΚΕΝΤΡΟ ΤΕΚΜΗΡΙΩΣΗΣ NATIONAL DOCUMENTATION CENTRE

Bulletin of the Geological Society of Greece

Vol. 43, 2010

AMELIORATING THE SPATIAL RESOLUTION OF HYPERION HYPERSPECTRAL DATA. THE CASE OF ANTIPAROS ISLAND

Nikolakopoulos K.	Institute of Geology and Mineral Exploration,
Gioti Ev.	Department of Geography, Harokopio University of Athens
Skianis G.	University of Athens, Department of Geology and Geoenvironment
Vaiopoulos D.	University of Athens, Department of Geology and Geoenvironment

https://doi.org/10.12681/bgsg.11337

Δελτίο της Ελληνικής Γεωλογικής Εταιρίας, 2010
Πρακτικά 12ου Διεθνούς Συνεδρίου
Πάτρα, Μάιος 2010

Bulletin of the Geological Society of Greece, 2010
Proceedings of the 12th International Congress
Patras, May, 2010

AMELIORATING THE SPATIAL RESOLUTION OF HYPERION HYPERSPECTRAL DATA. THE CASE OF ANTIPAROS ISLAND

Nikolakopoulos K.[1], Gioti Ev.[2], Skianis G.[3], and Vaiopoulos D.[3]

[1] *Institute of Geology and Mineral Exploration, Olympic Village Entrance C, 13677 Acharnae Athens, Greece knikolakopoulos@igme.gr,*

[2] *Department of Geography, Harokopio University of Athens 70, El. Venizelou Str, Athens 17671 Greece, gs20505@hua.gr*

[3] *University of Athens, Department of Geology and Geoenvironment, 15784 Panepistimiopolis Zografou, Greece, skianis@geol.uoa.gr, vaiopoulos@geol.uoa.gr*

Abstract

In this study seven fusion techniques and more especially the Ehlers, Gram-Schmidt, High Pass Filter, Local Mean Matching (LMM), Local Mean and Variance Matching (LMVM), Pansharp and PCA, were used for the fusion of Hyperion hyperspectral data with ALI panchromatic data. The panchromatic data have a spatial resolution of 10m while the hyperspectral data have a spatial resolution of 30m. All the fusion techniques are designed for use with classical multispectral data. Thus, it is quite interesting to investigate the assessment of the common used fusion algorithms with the hyperspectral data. The study area is Antiparos Island in the Aegean Sea.

Key words: *Hyperion, Hyperspectral data, fusion, Antiparos Island.*

1. Introduction

The majority of the earth observing satellites such as SPOT, Landsat, Ikonos, Quickbird, EO-1 (ALI sensor) collect at the same time a panchromatic image with a higher spatial resolution and many multispectral bands with lower spatial resolution. This is due to technical reasons such as limited storage capacity, small data transfer rate and the limited energy autonomy of most of the satellites. These limitations affect more the hyperspectral sensors like Hyperion that collect more than 240 bands. Considering these limitations, it is clear that the most effective solution for providing high-spatial resolution hyperspectral remote sensing images is to develop effective image fusion techniques.

In this study seven fusion techniques and more especially the Ehlers, Gram-Schmidt, High Pass Filter, Local Mean Matching (LMM), Local Mean and Variance Matching (LMVM), Pansharp and PCA, were used for the fusion of Hyperion hyperspectral data with ALI panchromatic data. Both sensors are on onboard Earth Observing-1 satellite. Thus the data was collected simultaneously thus, there are no radiometric and atmospheric problems. The data was provided to IGME from USGS. The panchromatic data have a spatial resolution of 10m while the hyperspectral data have a spatial resolution of 30m. All the fusion techniques used in this study are designed for classical multispectral data and tested in previous studies (Chavez et al., 1991; Vaiopoulos et al., 2001; Nikolakopoulos, 2003; Aiazzi et al., 2002; Wang et al., 2005; Nikolakopoulos 2005; Laporterie-Dejean et al., 2005; Nikolakopoulos, 2008). Thus, it is quite interesting to investigate the assessment of the common used fusion algorithms with hyperspectral data.

2. Bands number reduction

The Hyperion data usually presents a low signal to noise ratio. Furthermore forty-six of the two hundred forty two Hyperion bands are uncalibrated so it is better not to be used. In order to reduce the total number of the bands a pre-selection based on optical and statistical criteria was done. Firstly, all the bands were examined visually. The optical control detected many bands dominated by noise and some other bands with no useful information (totally black or white images). Second, the histogram parameters of all the bands were examined. The statistical control of the minimum, maximum and the standard deviation values confirmed the existence of bands corrupted by noise. As a result only 155 bands (8-57, 78, 82-97, 99-119, 134-164, 182-184, 187-219) were used for the fusion processing. The spectral range of these bands is presented in Table 1.

3. Fusion techniques used in this study

The Ehlers algorithm (Ehlers, 2004; Ling et al., 2007; Ehlers et al., 2008) implemented in Erdas Imagine software is based on IHS transform and filtering in the Fourier Domain and should give the same quality results independently of the type of the images. The Gram Schmidt algorithm simulates a panchromatic band from the lower spatial resolution multispectral bands, performs a Gram-Schmidt transformation on the simulated panchromatic band and the multispectral bands, using the simulated panchromatic band as the first band, then swaps the high spatial resolution panchromatic band with the first Gram-Schmidt band and finally applies the inverse Gram-Schmidt transform to form the fused spectral bands. A limitation of the algorithm is that the low spatial resolution multispectral bands used to simulate the panchromatic band must fall in the range of the high spatial resolution panchromatic band or they will not be included in the resampling process (Laben and Brower, 2000; Envi, 2008).

The process of the High Pass Filter involves a convolution using a High Pass Filter (HPF) on the high resolution data, then combining this with the lower resolution multispectral data. More specially the algorithm read pixel sizes from image files and calculates the ratio of multispectral cell size to high-resolution cell size. Then it High-pass filter the high spatial resolution image, resample the multispectral image to the pixel size of the high-pass image and finally add the HPF image to each multi-spectral band. The HPF image is weighted relative to the global standard deviation of the multi-spectral band. The algorithm stretches the fused image to match the mean and standard deviation of the original multispectral image (ERDAS, 2008).

The LMM (Local Mean Matching) and the LMVM (Local Mean and Variance Matching), methods were specifically designed in order to minimize the difference between the fused image and the low-resolution MS channels (De Béthune et al., 1998), hence to preserve most of the original spectral information of the low-resolution channels. These filters apply normalization functions (Joly, 1986) at a local scale within the images in order to match the local mean and/or local mean and variance values of the PAN image with those of the original low-resolution spectral channel. The small residual differences remaining correspond to the high spatial information stemming from the high-resolution PAN image. This type of filtering drastically increases the correlation between the fused product and the low-resolution channel. By adjusting the filtering window sizes, the amount of spectral information preserved in the fused product can be controlled.

The Principal Component Analysis algorithm calculates principal components, remaps the high resolution image into the data range of PC-1 and substitutes it for PC-1, then applies an inverse principal components transformation. The Principal Component method is best used in applications that require the original scene radiometry (color balance) of the input multispectral image to be maintained as

Table 1.

Spectral bands no	**Spectral Length (nm)**	**Full Width at Half the Maximum FWHM (nm)**
8	426,82	11,38
57	925,41	11,27
78	922,54	11,04
82	962,91	11,04
97	1114,19	10,95
99	1134,38	10,92
119	1336,15	10,69
134	1487,53	11,04
164	1790,19	11,45
182	1971,76	10,93
184	1991,96	10,91
187	2022,25	10,90
219	2345,11	10,40

closely as possible in the output file. As this method scales the high resolution data set to the same data range as Principal Component 1, before the Inverse Principal Component calculation is applied, the band histograms of the output file closely resemble those of the input multispectral image.

The Pansharp fusion technique proposed by (Zhang, 1999) seems to have solved the two major problems in image fusion – colour distortion and operator dependency. A method based on least squares was employed for a best approximation of the grey value relationship between the original multispectral, panchromatic, and the fused image bands for a best colour representation. Statistical approaches were applied to the fusion for standardizing and automating the fusion process.

Some of the algorithms used in this study allow for various parameter settings. So many different tests were done. For every algorithm the best visual result was selected for the quality assessment. In all cases, the nearest neighborhood resampling method was applied.

For each fused image the following issues have been examined: a) the visual qualitative result, b) the statistical parameters of the histograms of the various frequency bands c) the correlation coefficient and d) the entropy of the original bands to the respective entropy of the fused bands was compared. Those criteria are in accordance with the general quality assessment criteria that were described in previous studies (Wald et al., 1997; Chavez et al., 1991).

4. Comparing the quality of seven fused images with the original Hyperion image

4.1. Visual Comparison

As already mentioned in this study, the quality of the fusion algorithms was evaluated both qualitatively and quantitatively. Visual comparison of all the possible band combinations of the fused images was used for the qualitative assessment, since it is the most simple but effective tool for showing the major advantages and disadvantages of a method.

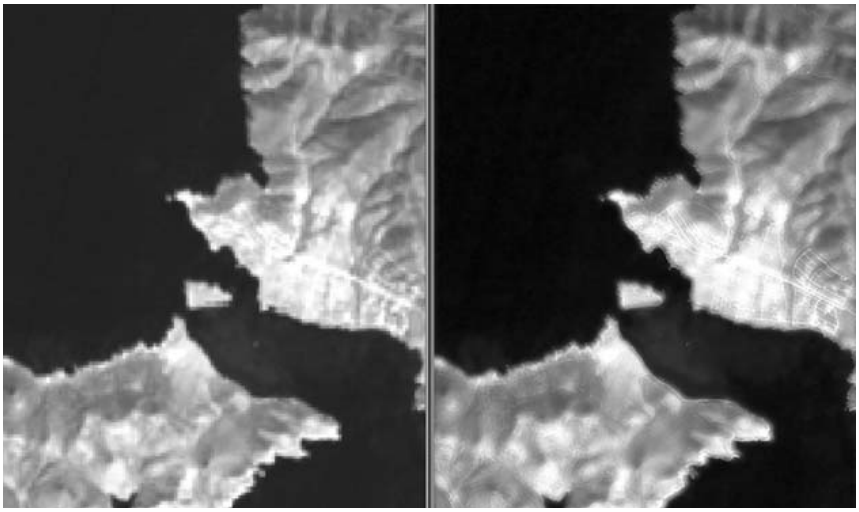

Fig. 1: (left): The original Hyperion image at 1/25.000 scale. A RGB combination of specific bands (2203, 844, 487 nm) is presented; (right): The same RGB combination of the Ehlers fused image.

Fig. 2: (left): The Gram-Schmidt fused image at 1/25.000 scale. A RGB combination of specific bands (2203, 844, 487 nm) is presented; (right): The same RGB combination of the HPF fused image.

A RGB combination of specific bands (2203, 844, 487 nm) of the original and the fused images are presented below (Figs 1-4). A first remark is that all the fusion algorithms ameliorate the spatial resolution of the original Hyperion data. The road network, the fields, the river network and the coastline can be more easily detected and mapped in the fused images. More particularly, the Ehlers fused image presents a much better spatial resolution, as some of the most important geomorphological characteristics can be easily discriminated. Moreover, it is obvious that the quality of the colours has been enhanced. Nevertheless, the contrast failed to give any better result. The Gram Schmidt fused image presents also a better spatial resolution. In that image, even the morphology of the sea bottom can be observed, which mean that bathymetrical information can be derived. Furthermore, there is a small amelioration in the contrast and a change in the quality of its colours as they became darker. Observing the HPF fused image, it can be easily seen that its spatial resolution is quite sat-

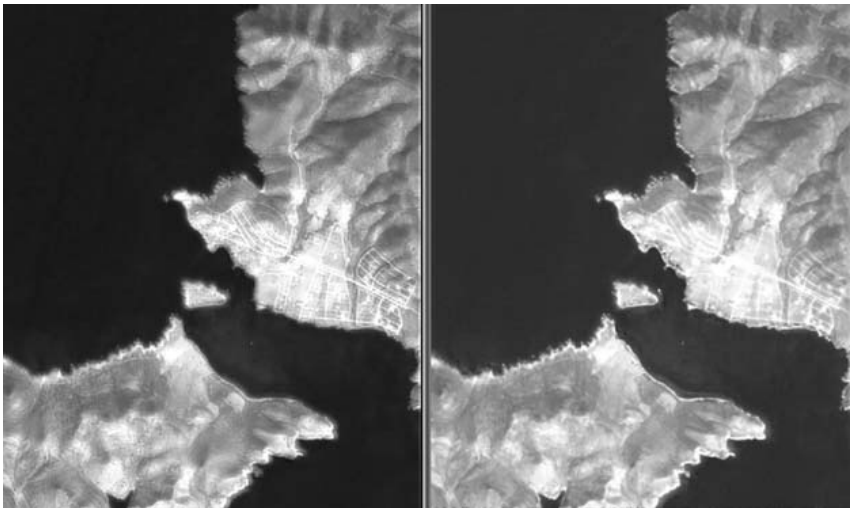

Fig. 3: (left): The LMM fused image at 1/25.000 scale. A RGB combination of specific bands (2203, 844, 487 nm) is presented; (right): The same RGB combination of the LMVM fused image.

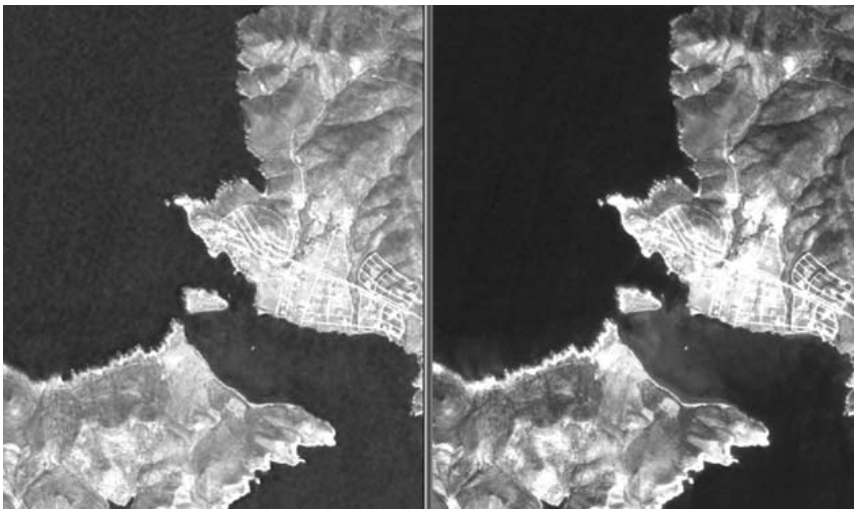

Fig. 4: (left): The Pansharp fused image at 1/25.000 scale. A RGB combination of specific bands (2203, 844, 487 nm) is presented; (right): The same RGB combination of the PCA fused image.

isfied, comparing with Hyperion's. This image gives information about the road network, every field, the vegetation; even the coast line can be discriminated. The contrast of the image also presents a great enhancement but the quality of the colours isn't so representative. The LMM and the LMVM fused image also present better spatial resolution. They generally preserved the original colours and present a better contrast. The Pansharp fused image even if has also better spatial resolution than Hyperion's, doesn't give any further information about the morphology of the sea bottom. Moreover, the quality of the colour has changed and the contrast is presented with better results. The PCA fused image, has also a really satisfying spatial resolution as all the basic elements of the area, such us road network and vegetation are being illustrated. Bathymetrical information can also be retrieved. Meanwhile, the quality of the colour has been changed and now seems to be little darker and the contrast is at a better level.

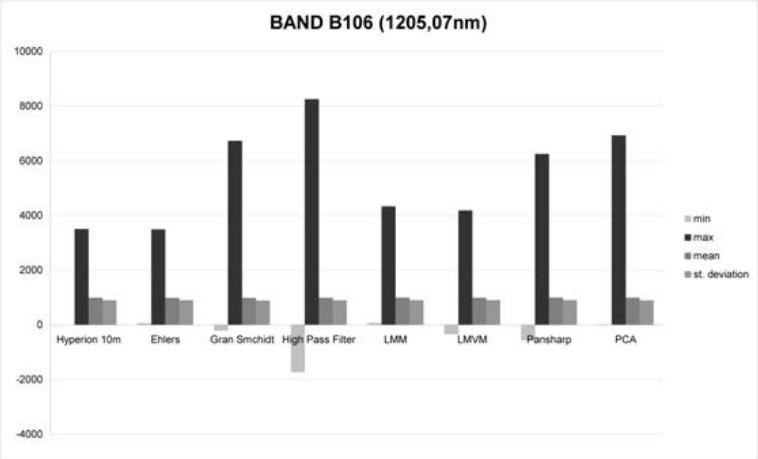

Fig. 5: The statistical parameters of the Hyperion band B106 and the respective fused bands.

4.2. Statistical Comparison

For all the images the statistical parameters of the histogram and especially the standard deviation of some specific bands were studied. The value of the standard deviation is vital in recognizing different unities. The higher the value of the standard deviation of a histogram is, the more different formations can be recognized. The statistical control is necessary in order to examine spectral information preservation. When the researcher wants to proceed to digital processing of the data (for example applying different ratios for mineral detection), an alteration to the original spectral characteristics wouldn't be appropriate, as it may influence the results.

As it can be observed all the fusion techniques didn't provoke significant changes to the standard deviation and the mean values (Fig. 5 and Fig. 6). There are only some changes at the value of minimum and maximum.

Particularly, it has to be pointed out that the Ehler's algorithm increases the minimum value of the bands 14, 21, 31, 41, 49, 55 and 87. The rate of the increase slows down for the bands 106,116,136 and 151 and finally there is no change for the minimum value of the bands 161,195,205,218. At the maximum value of this algorithm it can't be distinguished any significant alteration.

The Gram Schmidt algorithm has also some variations at the minimum value, which are higher at bands 14, 21, 31. The maximum value differs from Hyperion's in all bands and there is a big difference at band 87. About the High Pass Filter fusion technique, the minimum value has changed in all cases and entails a negative number. The minimum value for the bands 49, 87, 106 has the greatest fluctuation from the others. The maximum value of this technique presents the same inclination with the one of Gram Schmidt where there were some remarkable changes in all bands and band 87 had the higher deviation. It is quite interesting to observe the LMM technique, which has the smallest changes in the minimum value comparing with the other algorithms. Only bands 14, 21, 31, 41, 49, 55, 87, 106, 116, 136, 151, present a negligible alteration and at the bands 161, 195, 205, 218 the value remains the same. The maximum value has also some negligible changes at lower bands and at higher bands there isn't any fluctuation at all. The LMVM algorithm has the same behaviour for the minimum values in all bands which mean that there is a small variation in all cases and all the values appears to have negative numbers. The maximum value only entails some small differences. The Pansharp technique presents a small deviation at the minimum value, which is almost at the same range. It is important to be marked that bands 14, 21, 31, 41 entail a positive number and the rest bands have a negative one. The maximum value presents some alteration in all bands. Band

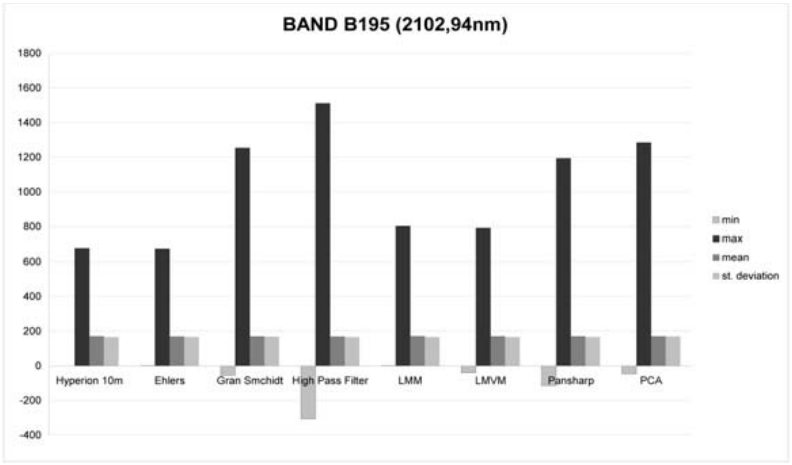

Fig. 6: The statistical parameters of the Hyperion band B195 and the respective fused bands.

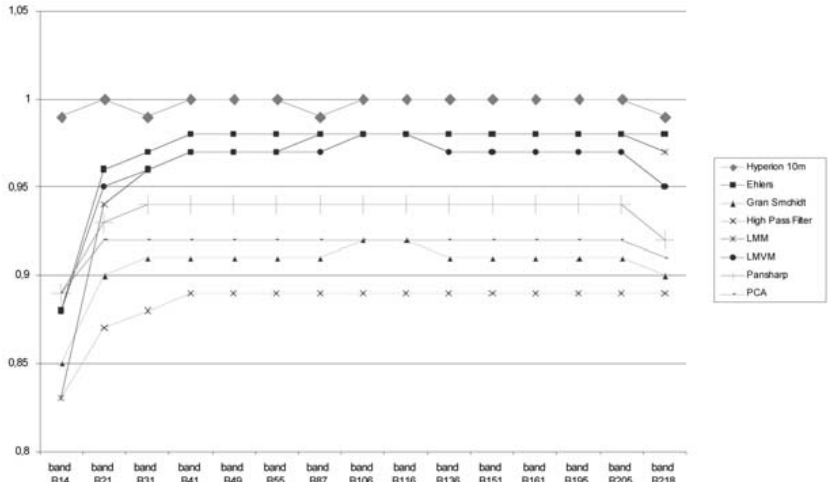

Fig. 7: The correlation value of specific fused bands and the respective original Hyperion bands.

14 has the smallest and band 87 has the biggest. Finally, PCA algorithm provokes some variations in the minimum value. Bands 106 to 218 present the smallest alteration. The maximum value also entails changes which are higher at band 87.

4.3. Correlation

The closeness between two images can be quantified in terms of the correlation function. The correlation coefficient ranges from -1 to 1. A correlation coefficient value of -1 indicates that the two images are highly correlated, i.e., very close to one another. A correlation coefficient of -1 indicates that the two images are exactly opposite to each other.

Each band of the original hyperspectral image has been correlated with the respective fused band. The correlation coefficients have been computed. The best spectral information is available in the hyperspectral image and hence the fused image bands should have a correlation closer to that of the hyperspectral image bands. The results are presented above (Fig. 7).

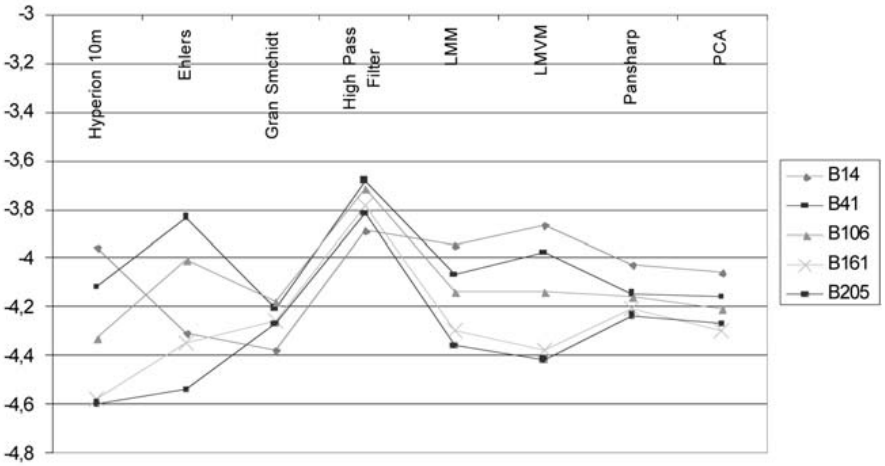

Fig. 8: The entropy of the Hyperion bands B14, B41, B106, B161, B205 and the respective fused bands.

The Ehlers fused image with a value close to 0,98 presents the highest correlation. The LMM and LMVM fused images have also a very satisfied correlation which it is close to 0,97. The High Pass Filter fused image presents the lower correlation to the original data. Its values are between 0,83 and 0,89. It is quite interesting to underline that all the fusion algorithms present the lower correlation values for the bands B14 and band B21. For the bands B31 to B205 the correlation is being increased. After the band 205 it can be observed that there is a decreasing tendency.

4.4 Entropy

The entropy H of an image may be defined:

$$H = \sum_{i=0}^{L} p_i \cdot \ln p_i$$

p_i is the percentage of the pixels of the image with digital number *i*. L is the quantization level (tonality range) of the image. For example if the digital number may take 28 different integer values from 0 to 255, L is equal to 255.

The entropy is generally considered to be a measure of the information content of the image. As long as the width of the image histogram increases, H also increases. Skewed image histograms have bigger entropy than symmetrical ones with the same standard deviation (Skianis & Nikolakopoulos 2008). Therefore the entropy value of a digital image contains information about the standard deviation and the shape of the histogram.

Observing band 14 (Fig. 8) it can be seen that High Pass Filter and LMVM fused images increase the entropy, LMM gives almost the same result with Hyperion's and all the other fusion techniques present a decrease in the entropy. The highest increase is presented in the high pass filter technique and the highest decrease in the Gram Schmidt. In Band 41 there are also some variations in the entropy as three of the fused images presents an increase (Ehler's, High Pass Filter and LMVM), three didn't give any fluctuation and two present a decrease from which Gram Schmidt's gives the greatest. About bands 106, 161 and 205 it can be observed that all the fused images present an increase in the entropy from which High Pass Filter has the highest and PCA the lowest. It would be inter-

esting to underline that High Pass Filter algorithm presents an important increase in all bands. Moreover, it can be observed that only bands 14 and 41 presented a decrease in certain fused images. All other bands give an increase in the entropy.

5. Conclusions

Seven fusion algorithms designed for multispectral data were tested on Hyperion hyperspectral data. The initial spatial resolution of Hyperion data (30m) has been ameliorated and the finally fused images have a spatial resolution of ten meters (10m). All the algorithms improve the target detectability of the Hyperspectral data. The road network, the fields and generally the formation boundaries can be more easily detected and mapped. All the algorithms keep almost invariable the mean and the standard deviation values of the original data. All the algorithms with the exception of the High Pass Filter provoke minor changes to the minimum value and a significant increase to the maximum value of the original data. All the fused images present a very high correlation to the original Hyperion bands. All the algorithms enhance the information contained in the original image as they increase the entropy value of most of the Hyperion bands.

The general conclusion is that the specific algorithms even if they were designed for use with classical multispectral data they can be used for the fusion of Hyperion Hyperspectral data.

6. References

Aiazzi B., Alparone L., Baronti S. & Garzelli A., 2002. Context-Driven fusion of high spatial and spectral resolution images based on oversampled multiresolution analysis, *IEEE Transactions On Geoscience And Remote Sensing*, vol. 40, No. 10, October 2002, p. 2300-2312.

Chavez, P.S. Jr., Sides, S.C., Anderson, J.A., 1991. Comparison of three different methods to merge multiresolution and multispectral data : Landsat TM and SPOT Panchromatic, *Photogrammetric Engineering and Remote Sensing*, Vol. 57, N° 3, pp. 295-303.

De Bethune S., Muller F.,, Donnay J.P., 1998. Fusion Of Multispectral And Panchromatic Images By Local Mean And Variance Matching Filtering Techniques, *Fusion of Earth Data*, Sophia Antipolis, France, 28-30 January 1998.

Ehlers M., 2004. Spectral characteristics preserving image fusion based on Fourier domain filtering, *Proc. of SPIE* Vol. 5574 p. 1-13.

Ehlers M., Klonus S., Astrand P.J., 2008. Quality assessment for multi-sensor multi-date image fusion, *Proc. XXIth Int. Congr. ISPRS*, Beijing, China p. 499-506.

Envi, 2008. *Envi User's Guide Version 4.5* 2008,p 1152.

Erdas, 2008. *Erdas Field Guide* p. 770.

Joly, G., 1986. *Traitements des fichiers images*, Collection Télédetection satellitaire, No. 3, Paradigme, Caen, 137 p.

Laporterie-Dejean F., De Boissezon H., Flouzat G., & Lefevre-Fonollosa M., 2005. Thematic and statistical evaluations of five panchromatic/multispectral fusion methods on simulated pleiades-hr images, *Information Fusion*, vol. 6, no. 3, pp. 193–212.

Laben, C. A., Brower B. V., 2000. Process for Enhancing the Spatial Resolution of Multispectral Imagery Using Pan-Sharpening, US Patent 6,011,875.

Ling Y., Ehlers M., Usery L., Madden M., 2007. FFT-enhanced IHS transform method for fusing high resolution satellite images, *ISPRS Journal of Photogrammetry & Remote Sensing* 61, 381-392.

Nikolakopoulos K., 2003. Comparative study of fusing ETM data with five different techniques for the

broader area of Pyrgos, Greece, *Proc of SPIE*, Vol. 5238, p. 84-95.

Nikolakopoulos K., 2005. Comparison of six fusion techniques for SPOT5 data, *IEEE 2005 International Geoscience and Remote Sensing Symposium*, Seoul Korea 25-29 July 2005. Vol. 4, p. 2811- 2814.

Nikolakopoulos K., 2008. Comparison of Nine Fusion Techniques for Very High Resolution Optical Data, *Photogrammetric Engineering & Remote Sensing*, Vol. 74 No 5, May 2008, pp.647-659.

Skianis, G., Nikolakopoulos, K., 2009. The entropy as a measure of the performance of the NDVI vegetation index-a pilot study with an ALOS digital image. *Proc. of 'ALOS PI 2008 Symposium*", Island of Rhodes, Greece 3–7 November 2008, ESA SP-664, January 2009. Unpaginated CDRom.

Vaiopoulos D., Nikolakopoulos K., Skianis G., 2001. A comparative study of resolution merge techniques and their efficiency in processing images of urban areas. *IEEE/ISPRS Joint Workshop on Remote Sensing and Data Fusion over Urban Areas*, Rome, Italy, November 8-9th, 2001,p. 270-274.

Wald, L., Ranchin, Th., Mangolini, M., 1997. Fusion of satellite images of different spatial resolutions: Assessing the quality of resulting images, *Photogrammetric Engineering and Remote Sensing*, Vol. 63,N° 6, pp. 691-699.

Wang Z., Ziou D., Armenakis C., Li D., and Li Q., 2005. A comparative analysis of image fusion methods, *IEEE Transactions on Geoscience and Remote Sensing*, vol. 43, no. 6, pp. 1391–1402.

Zhang, Y., 1999. A new merging method and its spectral and spatial effects, *International Journal of Remote Sensing*, vol. 20, pp. 2003-2014.